URSI GASS 2021, Rome, Italy, 28 August - 4 September 2021

Simulation and Analysis for Electromagnetic Environment of Traction Network

Lu Zhang(1), Yun Zhu(1), Song Chen* (1), and Dan Zhang(1)
(1) Beijing Jiaotong University, Beijing, China

Abstract

Due to the hidden safety hazards in the traction network of electrified railways in windy areas in China, it is necessary to study the influence of the protective wire landing on the traction backflow and power frequency magnetic fields. Therefore, in this paper, based on the theory of Multi-conductor Transmission Lines (MTL), a mathematical model of traction network is established to study the current distribution in each return conductor before and after the protective wire falls to the ground. The finite element method is used to establish a simulation model of the traction network under the normal working condition and the short-circuit fault condition of the contact wire and rail. The power frequency magnetic field generated by the railway traction network along the railway is simulated, and the influence of position of the protection line to the magnetic environment distribution along the railway is analyzed.

1 Introduction

The main line of the Lanzhou-Xinjiang high-speed railway in China is 1776 km in length. The train will pass through five windy regions in Gansu and Xinjiang. The wind season often causes traffic interruption, bringing huge losses to railway transportation [1]. The protective wire (PW) is an important part of the traction network. It is connected in parallel with the rail to provide a path for current, so as to reduce the rail potential and facilitate relay protection. Because the PW is a slender flexible structure, it is easy to causing hazards such as short circuit or fatigue disconnection under the action of wind, which affects the safe operation of the train. Earlier literatures studied the power frequency electromagnetic field of electrified railways by mirror image method or finite element method. In [2], mirror image method is used to solve the electric and magnetic field distributions of DC contact network. The finite element method is used to calculate the power frequency electromagnetic field distribution of the traction network [3, 4].

In view of this, this article models and calculates the distribution law of traction return current and power frequency magnetic fields under normal power supply and short-circuit fault conditions of the autotransformer (AT) traction network before and after PW landing. The safety of the magnetic environment along the railway line is comprehensively evaluated, which provides a basis for the line design and environmental impact in windy areas.

2 Mathematical Model of High-speed Railway Traction Network

2.1 Traction Network Structure of AT Power Supply Mode

The traction power supply system of the AT power supply mode is composed of a traction substation (SS) and a traction network. The structure of the traction net and the spatial position of each wire are shown in Figure 1. The multi-conductor system consists of contact wire (CW), catenary (MW), positive feeder (F), rail (R), protective wire (PW), and through ground wire (GW), etc. PW_L in the picture is the protective wire after landing. The parameters of each wire of the traction net are shown in Table 1.

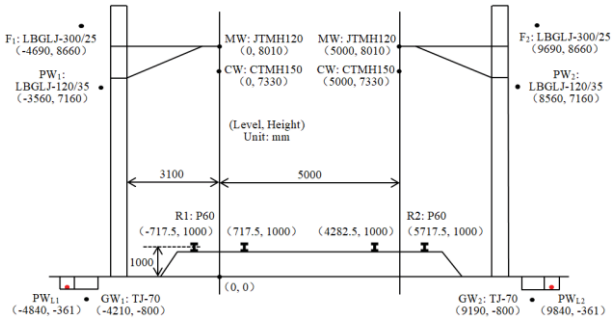

Figure 1. AT power supply traction network structure diagram.

Table 1. Parameters of each wire of AT power supply traction network.

	CW	MW	R	PF	PW	GW
Radius (mm)	7.2	7.0	49.5	11.88	8.12	5.25
resistance (Ω/km)	0.18	0.24	0.03	0.09	0.21	0.27

2.2 Traction Network Chain Network Model

The contact wire and the catenary on the same line side are equivalent to the T line, and the rails on the same line side are equivalent to the R line, so that the traction net is simplified into 10 wires. By cutting the traction network

to a specific length, a chain network model of traction network with full parallel AT power supply mode is established on the basis of maintaining its distribution parameter characteristics [5, 6]. This model divides the traction network into longitudinal series elements and transverse parallel elements. These elements are appropriately modeled, so that the whole traction network is equivalent to a chain network model, as shown in Figure 2.

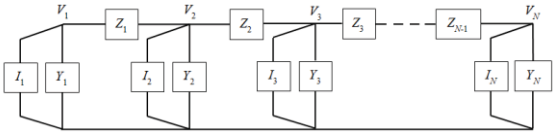

Figure 2. Traction network chain network model.

Assuming that the number of conductors is n and the entire feeding section is cut into N parts, the series impedance element $\boldsymbol{Z}$ is a branch impedance matrix between two adjacent cut planes, the parallel admittance element $\boldsymbol{Y}$ is the admittance matrix between the conductors on each cutting plane, and I is the injected current source vector of each conductor on the cutting plane. In the model shown in Figure 3, for the node i:

$$V_i - V_{i-1} = Z_i I_i^*. \tag{1}$$

The unit length impedance matrix and admittance matrix of the wire are calculated by using Carson formula and electrostatic field mirror method. Then the node voltage equation of the whole chain network circuit is solved to obtain the wire node voltage matrix. Substituting into equation (1) can obtain the wire current matrix of each segment, and the entire network is solved.

3 Calculation Results and Analysis of Traction Network Current

In this paper, the length of the feeding section is 30km, which is equally divided into two AT segments. The main parameters of the traction network are as follows: the traction substation adopts V_X connection traction transformer with rated voltage of 220/2×27.5kV, AT leakage impedance is 0.1+j0.45Ω, the grounding resistance is 0.5Ω, the ground resistivity is 100Ω·m, and the leakage resistance of the rail to ground is ignored. The rails, protective wires, and ground lines are completely transversely connected every 1.5km. The up and down rails are connected every 1.5km. The protective wires and ground lines are simply transversely connected every 500m. A feeding section is equally divided into 20 segments, and a distributed parameter module is used every 1.5km to establish a chain network model of the traction network.

3.1 Current Distribution of Traction Network under Normal Conditions

Assume that one side of a feeding section has only one load. In MATLAB, the steady-state current of the locomotive under normal operating conditions is set to 1000A, and it is located 6km from the traction substation in the first AT section of the uplink. Taking the traction substation as the coordinate origin, and the direction from the traction substation to the section post is the positive return direction. The current distribution of each conductor in the traction network can be obtained, as shown in Figure 3. Similarly, when PW is landed, the current distribution of each wire of the traction network after PW landing is simulated in MATLAB, as shown in Figure 4.

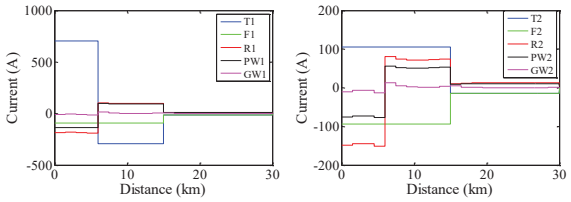

Figure 3. Current distribution of each wire under normal conditions.

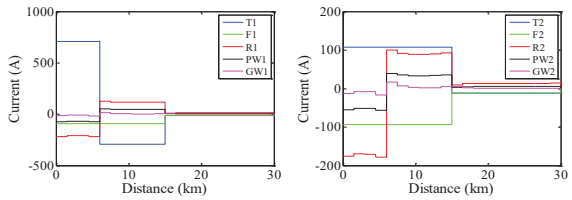

Figure 4. Current distribution of each wire after PW landing under normal conditions.

Comparing Figure 3 and Figure 4, it can be found that after the PW falls to the ground, the rail current ratio of the uplink and downlink lines increased by 5.10% and 4.66%, and the protective wire current ratio of the uplink and downlink lines decreased by 10.90% and 3.67%, respectively. The current ratio of ground wire increased by 0.76%, and the proportion of current in the ground increased by 3.29%. Compare the traction return current ratio of rail, protective wire, and ground wire before and after the PW falls to the ground, as shown in Figure 5. The current in rail and ground wire increase when the protection wire falls to the ground, and the current in the protective wires decrease.

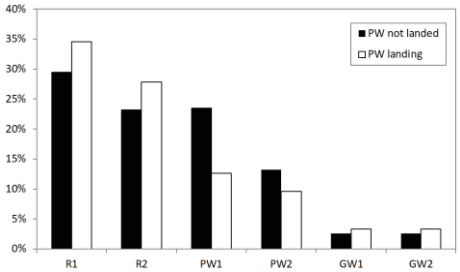

Figure 5. The proportion of traction return current before and after PW landing.

3.2 Current Distribution of Traction Network under T-R Short Circuit Fault

In MATLAB, the T-R short-circuit current is set to 5000A, T1 and R1 are shorted, and the short-circuit point is located 6km from the traction substation in the first AT section. The current distribution of each conductor of the traction network can be obtained, as shown in Figure 6. Similarly, when PW is landed, the current distribution of each wire of the traction network after PW landing is simulated in MATLAB, as shown in Figure 7.

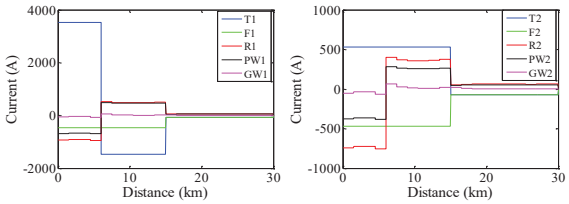

Figure 6. Current distribution of each wire under T-R short circuit fault.

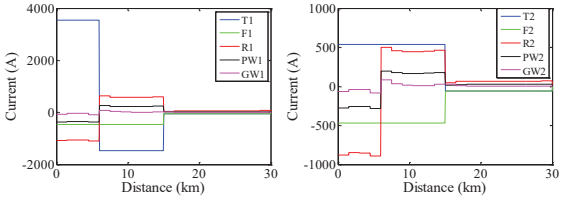

Figure 7. Current distribution of each wire after PW landing under T-R short circuit fault.

Comparing Figure 6 and Figure 7, it can be found that after the PW falls to the ground, the rail current ratio of the uplink and downlink lines increased by 5.10% and 4.66%, and the protective wire current ratio of the uplink and downlink lines decreased by 10.91% and 3.67%, respectively. The current ratio of ground wire increased by 0.76%, and the proportion of current in the ground increased by 3.30%. Therefore, after the PW falls to the ground, the T-R short-circuit fault of the traction network is basically the same as the distribution change of traction return current under normal power supply.

4 Calculation and Analysis of Power Frequency Magnetic Field in Traction Network

Ansys Maxwell software is used to simulate the two-dimensional power frequency magnetic field of the traction network along the railway. Aiming at the influence of power frequency magnetic field on sensitive equipment along the railway line, taking signal cables as an example, in order to ensure its normal operation, the standard GB/T 24338.5-2018 [7] is taken as the limit standard for electromagnetic radiation of equipment. The power frequency magnetic field limit of a 50Hz AC traction system is 100A/m.

4.1 Simulation Analysis of Magnetic Field under Normal Power Supply of Traction Network

Based on the two-dimensional model of the traction network shown in Figure 1, the current distribution of each conductor on the side of the traction substation obtained in Section 3.1 is used as the excitation condition. Under normal power supply of the traction network, magnetic induction intensity of traction substation side at the load before and after PW landing is obtained, as shown in Figure 8.

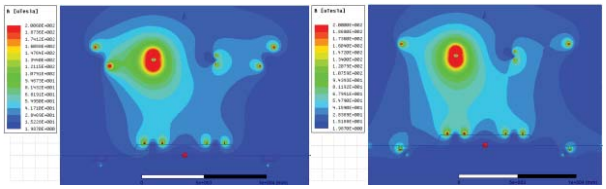

Figure 8. Magnetic field distribution on the side of the traction substation before and after PW landing.

Analysis of Figure 8 shows that when PW does not fall to the ground, at the signal cable trough of the traction network, the maximum value of the magnetic induction intensity on the running side is about 14.24μT, and the non-operation side is about 10.16μT. After PW landed, the maximum value of the magnetic induction intensity on the running side is about 83.15μT, and the non-operational side is about 65.15μT. It can be seen that the PW landing increases the magnetic induction intensity at the signal cable trough, but it does not exceed the standard limit of 100A/m, about 125.63μT.

4.2 Simulation Analysis of Magnetic Field under T-R Short Circuit Fault of Traction Network

Taking the short-circuit current distribution of each conductor obtained in Section 3.2 as the excitation condition, the magnetic induction intensity of traction substation side at the short-circuit point before and after PW landing is obtained, as shown in Figure 9.

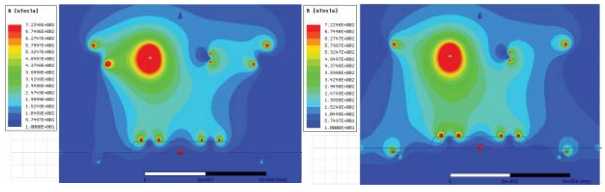

Figure 9. Magnetic field distribution on the side of the traction substation before and after PW landing.

Analysis of Figure 9 shows that when PW does not fall to the ground, at the signal cable trough, the maximum value of the magnetic induction intensity on the running side is about 69.71μT, and the non-operation side is about 51.66μT. After PW landed, the maximum value of the magnetic induction intensity on the running side is about 437.48μT, and the non-operational side is about 351.64μT. It can be seen that the PW landing increases the magnetic induction intensity at the signal cable trough, and it exceeds the standard limit of 100 A/m. Compare the change of power frequency magnetic field at the signal cable trough before and after the protective wire lands, as shown in Figure 10.

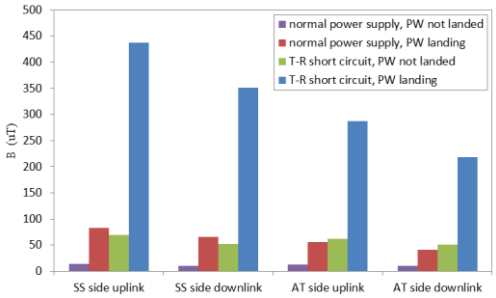

Figure 10. Power frequency magnetic field at the signal cable trough before and after PW landing.

The magnetic induction intensity generated by each wire of the traction network is proportional to the current and inversely proportional to the distance. The return current in rail and ground wire increase when the protection wire falls to the ground, the current in the protective wire decrease, and the distance between the protective wire and cable trough is the closest. Therefore, as shown in Figure 10, after the protective wire lands, the magnetic induction intensity at the signal cable troughs of the uplink and downlink lines increases both on the traction substation (SS) side and the autotransformer post (ATP) side.

5 Conclusion

In this paper, the Multi-conductor Transmission Line theory is used to calculate the current distribution in each return wire before and after PW landing. Then the finite element method is used to calculate the power frequency magnetic field under the condition of normal power supply and T-R short circuit fault of the traction network, and the influence of PW landing on the magnetic field environment distribution along the railway is studied.

Under the normal power supply and the T-R short-circuit fault of the traction network, the return current in rail and ground wire increase when the protection wire falls to the ground, the current in the protective wire decrease, the magnetic induction intensity at the signal cable trough increases. Under the normal power supply of the traction network, the influence of the power frequency magnetic field on the equipment does not exceed the standard limit of 100A / m, but it exceeds the standard limit in the case of a T-R short-circuit fault. It can be considered to adjust the landing position of the protective wire from the design perspective, or limit the short-circuit current of the traction network and shorten the short-circuit removal time of the relay protection to reduce the magnetic impact on the signal equipment along the line.

6 Acknowledgements

This work is supported by the basic scientific research business expenses of Beijing Jiaotong University (No. 2020JBZD010), and the Pre-research on National Major Projects of Sichuan-Tibet Railway (No. 2019CZ001).

7 References

1. Han Jiadong, “Study on Galloping Mechanism and Protective Measures of Additional Conductors of High-speed Railway Catenary in windy Area,” *Railway Standard Design*, **59**, 12, December 2015, pp.125-129, doi:10.13238/j.issn.1004－2954.2015.12.029.

2. Apollonskii S. M., Gorsky A. N., “Calculation of electromagnetic field strengths produced by a direct current traction network,” *EUROCON 2019*, May 2009, pp.873-880, doi:10.1109/EURCON.2009.5167737.

3. Buccella C., Feliziani M., “Three dimensional magnetic field computation inside a high speed train with a.c. electrification,” *IEEE International Symposium on Electromagnetic Compatibility*, May 2003, pp.617-620, doi:10.1109/ICSMC2.2003.1428334.

4. Sun Huijuan, Liu Jun, Huang Xingde, and Jiang Lei, “Numerical Simulation and Analysis of Electromagnetic Environment in Traction Power Supply Network of High Speed Railway,” *Electric Power*, **48**, 11, November 2015, pp. 60-66, doi:1004-9649(2015)11-0060-07.

5. Wei Wei, Liu Wei, and Ye Xiaowen, “Modeling and Analysis of Traction Return System for High Speed Railway,” *Journal of Railway Science and Engineering*, **15**, 1, January 2018, pp. 31-38, doi:1672-7029(2018)01-0031-08.

6. Wu Mingli, “Study on Electrical Parameters and Mathematical Model of Traction Power Supply System,” PhD, Beijing Jiaotong University, Beijing, 2006.

7. GB/T 24338.5-2018. Electromagnetic compatibility of railway applications Part 4: Emission and immunity of signal and telecommunications apparatus, National Bureau of Standards, Beijing, 2018.